Analytica Chimica Acta 1191 (2022) 339375

Contents lists available at ScienceDirect

Analytica Chimica Acta

journal homepage: www.elsevier.com/locate/aca

Dry-reagent microfluidic biosensor for simple detection of NT-proBNP via Ag nanoparticles

Franziska Beck [a], Carina Horn [b], Antje J. Baeumner [a, *]

[a] University of Regensburg, Institute of Analytical Chemistry, Chemo- and Biosensors, 93043, Regensburg, Germany
[b] Roche Diagnostics, 68305, Mannheim, Germany

HIGHLIGHTS

- Homogeneous flow assay without pre-incubation with on-chip dried reagents.
- NT-proBNP is detectable in a clinical relevant range via microfluidic analysis.
- Trehalose matrix with oxygen scavenger enables AgNP storage in dry form.

GRAPHICAL ABSTRACT

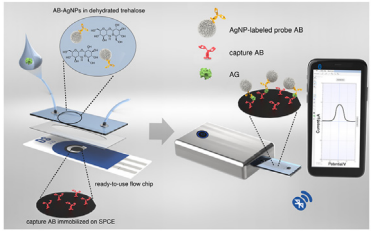

ARTICLE INFO

Article history:
Received 9 June 2021
Received in revised form
6 December 2021
Accepted 10 December 2021
Available online 12 December 2021

Keywords:
Electrochemical biosensor
Silver nanoparticle
Microfluidic
Blood analysis
Differential pulse voltammetry

ABSTRACT

The diagnosis of many diseases requires monitoring of biomarker levels over a period of time instead of assessing their concentration only once. For example, in case of heart failure determination, the levels of N-terminal prohormone brain natriuretic peptide (NT-proBNP) in blood vary so strongly amongst individuals, that the current procedure of one-time measurement in combination with clinical examination does not allow for accurate assessment of disease severity and progression. Our microfluidic biosensor addresses key characteristics of desirable home-tests which include low limits of detection, small sample volume (less than 10 μL), simple detection strategies, and ready-to-go all-dried long-term stable reagents. Here, electrochemically superior silver nanoparticles (AgNP) were dried directly within the microfluidic channel in a matrix of trehalose sugar doped with Na_2SO_3 as oxygen scavenger. This successfully prevented AgNP oxidation and enabled dry and ready-to-use storage for at least 18 weeks. Based on this, laser-cut flow chips were developed containing all bioassay reagents needed in a ready-to-go dry format. An oxidation-reduction stripping voltammetry strategy was used for highly sensitive quantification of the AgNPs as electrochemical label. This microfluidic biosensor demonstrated limits of detection for NT-proBNP of 0.57 ng mL^{-1} with a mean error of 6% ($n \geq 3$) in undiluted human serum, which is below the clinically relevant cut-off of 1 ng mL^{-1}. This practical approach has the potential to substitute commonly used lateral-flow assays for various biomarkers, as it offers low patient sample volumes hence supporting simple finger-prick strategies well-known also for other electrochemical biosensors, and independence from the notorious variability in fleece fabrication.

1. Introduction

Heart failure (HF) is a “global pandemic affecting at least 26 million people worldwide” with rising tendency [1]. The American Heart Association defines HF as “a complex clinical syndrome that

* Corresponding author.
E-mail address: antje.baeumner@ur.de (A.J. Baeumner).

https://doi.org/10.1016/j.aca.2021.339375
0003-2670/

can result from any structural or functional cardiac disorder that impairs the ability of the ventricle to fill or eject blood" [2]. In terms of diagnosis, clinical examinations dominate and are often paired with a detection of the HF marker N-terminal prohormone brain natriuretic peptide (NT-proBNP). The precursor propeptide (proBNP) is secreted due to myocardial wall stress upon volume or pressure overload. It is cleaved enzymatically forming BNP and NT-proBNP and both peptides are released into the blood stream. While BNP lowers the cardiac output and central venous pressure, NT-proBNP is biologically inert [3]. Although both peptides are initially present in equal concentrations, the NT-proBNP level is higher, since it is solely cleared passively from the circulation (half-life of 120 min vs. 20 min, respectively). Therefore, NT-proBNP concentration in blood is commonly used instead of BNP as measure for severity and progression of HF [4]. The combination of one-time measurements of NT-proBNP with clinical examination is challenging [5], as this is not a definite evidence for HF, and its level depends additionally on age, gender, race, disease, severity, comorbidities and medication [3]. Therefore, it is difficult to assess one certain cut-off value, which is true for every patient, which makes a quantification of NT-proBNP concentration in blood necessary [6]. Up to now, the prognostically meaningful threshold used by physicians for chronic HF is approximately 1000 pg mL^{-1}. With a quantification of NT-proBNP levels over a longer period of time, a rising pattern could be identified in an early stage and predict an imminent negative outcome [4]. Therefore, at-home monitoring of NT-proBNP concentration in blood for patients at risk could be highly beneficial both for prevention and monitoring of therapy progress [7,8]. Primary prevention of HF would decrease the number of incidents, while the improvement of medical care would lead to an increased survival rate. The final aim is to reduce incidents, mortality and hospitalization [5].

For home monitoring, it is inevitable to have a minimal sample demand, no sample preparation and preferably no processing steps other than sample addition. It is proposed here that microfluidics combined with electrochemical detection fulfill these requirements and show an enormous potential for miniaturization and POC testing [9,10]. With respect to optimizing the sensitivity afforded by simple electrochemical transducers like the here used screen printed carbon electrode (SPCE), many researchers use nanomaterials, such as metallic nanoparticles either as surface coating for the electrode or as a label. They have unique (electro)chemical, physical and optical properties, because their high surface-to-volume ratio and the more exposed crystalline plains compared to the bulk material accelerate mass transport [11]. We have thus developed previously an electrochemical assay in which silver nanoparticles (AgNPs) serve as label [12]. The detection sandwich is immobilized on the working electrode (WE) of a SPCE. After covering of the three-electrode area with potassium chloride the presence of AgNPs on the electrode surface is measured by a sequence of oxidation and reduction reactions followed by differential pulse voltammetry (DPV) [13]. This method is superior to the galvanic exchange assay process demonstrated by the Crooks research group [3,14,15], because no gold coating of the working electrode is necessary and the process is less diffusion dependent.

This assay showed high sensitivity and robustness, but the format was not suitable for point-of-care. Therefore, this assay principle [12] was combined with microfluidics (Fig. 1) in order to automate and simplify the assay steps, and especially also to enable dry storage of all reagents, and increase sensitivity and reproducibility.

A prominent strategy of combining microfluidics and (electro) chemical analysis is the flow injection analysis (FIA), where a flow stream carries the analyte over the electrode surface [16]. FIA formats outperform the often time consuming and expensive standard

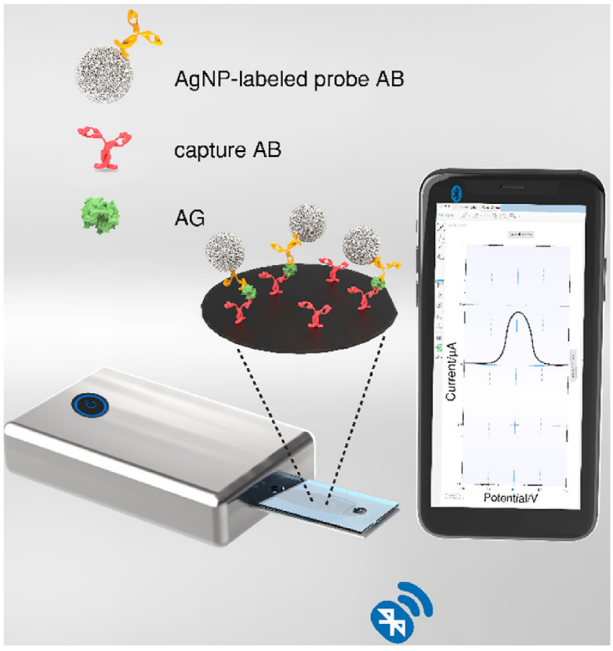

Fig. 1. Schematic (not-to-scale) representation of the sandwich assay on the WE of a SPCE integrated in a microfluidic chip with AgNPs as label using a Bluetooth potentiostat and a smartphone for the measurement. [Colors should be used in print]. (For interpretation of the references to color in this figure legend, the reader is referred to the Web version of this article.)

analytical methods because they offer quantitative information with high precision, sensitivity and reliability. Moreover, due to short analysis time and high sample throughput with minimal cost they are ideal for clinical analysis [11]. The here proposed simple microfluidic biosensorchip combines the LFA and FIA approaches with electrochemical detection and provides a strategy to include all reagents necessary in a dried format directly on chip (just as in an LFA) and use apply the pumping regime of a FIA system. Our unique set-up enables in contrast to other published work the formation of the detection complex in flow right on the working electrode. In contrast, in competing methods using AgNPs as labels [3,17] additional pipetting steps and/or wet chemicals are needed. In comparison to these others, our microfluidic assay can be used for home-monitoring, since it is simple to perform, *i.e.* no pipetting steps are necessary, and the chemicals can be stored in dry form over an extended time period. Of course, miniaturized pumps or strong capillary forces will in the future replace the pumps used within this work.

2. Experimental

2.1. Materials and instruments

Biotinylated capture antibody (polyclonal proBNP sheep-IgG-biotin), antigen (NT-proBNP (1-76) amid) in buffer or human serum and probe antibody (monoclonal NTproBNP mouse-IgG) were provided by Roche Diagnostics GmbH, Mannheim, Germany. Citrate capped silver nanospheres (d = 50 nm, 0.022 mg mL^{-1}) were purchased from nanoComposix (www.nanocomposix.com). Sodium chloride (NaCl, p.a), disodium hydrogen phosphate ($Na_2HPO_4 \cdot 2 H_2O$, p.a.), sodium hydrogen carbonate ($NaHCO_3$, p.a.) and potassium dihydrogen phosphate (KH_2PO_4, p.a.) were ordered from Merck (www.merckmillipore.com). Bovine serum albumin (BSA, >96%), trehalose (D-(+)-trehalose dihydrate, ≥99%), L-ascorbic acid (99%) and Tween 20 (>97%) were supplied from Sigma Aldrich (www.

sigmaaldrich.com). Potassium chloride (KCl, p.a.) was obtained from Roth (HYPERLINK "http://www.carlroth.com" \o "http://www.carlroth.com"www.carlroth.com). 4-(2-hydroxyethyl)-1-piperazineethanesulfonic acid (HEPES, ≥99%) and sodium sulfite (Na_2SO_3, p.a.) were acquired from VWR (de.vwr.com) and sodium hydroxide (NaOH, 1 M) was bought from Labochem international (www.labochem.de). Polyethyleneterephthalat (PET) foil was ordered from GoodFellow (HYPERLINK "http://www.goodfellow.com" \o "http://www.goodfellow.com"www.goodfellow.com). Double-sided adhesive tape (thickness = 100 μm) was purchased from Roeckelein GmbH (www.roeckelein-gmbh.de), while PMMA (Plexiglas® XT) was supplied from Kunststoff Acryl Design GmbH (www.kad-group.de).

HEPES buffer consisted of 10 mM HEPES and was adjusted to a pH of 7.4. HEPES blocking buffer was prepared by addition of 0.1% (w/v) BSA to this HEPES buffer. Phosphate buffered saline (PBS) consisted of 137 mM NaCl, 2.7 mM KCl, 38 mM $Na_2HPO_4 \cdot 2\ H_2O$ and 12 mM KH_2PO_4 with a pH of 7.4. For PBST washing buffer 0.05% (w/v) Tween 20 were added to this PBS. PBS blocking buffer consisted of PBS and 1% (w/v) BSA.

Electrochemical measurements were performed using screen-printed carbon electrodes (SPCE) bare (DRP-110) or with streptavidin coated working electrode (DRP-110STR, both: Metrohm AG, www.dropsens.com) and an EmStat blue potentiostat with corresponding software (PalmSens, www.palmsens.com). For nanoparticle modification, the ThermoMixer comfort (Eppendorf, online-shop.eppendorf.de) was used. Flow chips were prepared using a laser cutter model VLS2.30 with CO_2 laser (30 W, λ = 10.6 μm) from Universal Laser Systems, Arizona, USA. For plasma cleaning, the PlasmaFlecto 10 from Plasma Technology GmbH (Herrenberg, Germany) was used. The chip holder was manufactured in house and the LEGATO® 111 syringe pump, which was used for the microfluidic experiments, was purchase from kd Scientific (www.kdscientific.com).

2.2. Modification of silver nanoparticles

The silver nanoparticles were modified using a simple adsorption procedure, which was already optimized and the modified nanoparticles (AB-AgNPs) were characterized in a previous work [12]. Very briefly: a volume of 1 mL of AgNP solution (0.02 mg mL^{-1}) was centrifuged for 10 min at 10,000 g. The supernatant was discarded and the pellet resuspended in 1 mL 10 mM HEPES (pH 7.4) with 10 μg probe antibody (AB). After incubation at room temperature with gentle mixing (350 rpm) for 2 h in the dark, the nanoparticles were centrifuged once again for 10 min at 10,000 g. The supernatant was discarded and the pellet resuspended in 1 mL HEPES blocking buffer (10 mM HEPES + 0.1% (w/v) BSA, pH 7.4).

2.3. Drying of labeled probe antibody

Experiments with dried AB-AgNPs were performed using coated polymer disks. They were prepared by pipetting 20 μL of the respective solution on a PET support and drying for 1 h at 50 °C. For the disks without matrix, the AB-AgNP stock solution (20 μg mL^{-1} in 10 mM HEPES + 0.1% (w/v) BSA, pH 7.4) was diluted 1:2 with 10 mM HEPES buffer (pH 7.4), while a 40% (w/v) trehalose solution (in 10 mM HEPES, pH 7.4) was used for the dilution for trehalose disks. To measure the electrochemical activity after several days of storage in the fridge, the nanoparticles were rehydrated with 20 μL 10 mM HEPES buffer (pH 7.4) for 1 h at room temperature and 10 μL were dried on top of the WE of a DRP-110 at room temperature. Then, 50 μL 0.1 M KCl was added covering the three-electrode area and the electrochemical measurement was performed: after pretreatment with 1.25 V for 60 s and −0.8 V for 30 s, differential pulse voltammetry (DPV) was performed from −0.25 V to 0.25 V with t_{puls} = 50 ms, E_{step} = 10 mV, $E_{amplitude}$ = 80 mV, scan rate = 20 mV s^{-1}.

The trehalose content and drying was optimized with respect to lower water content and higher reproducibility. For the following experiments, a 20% (w/v) trehalose solution (in 10 mM HEPES, pH 7.4) was used for dilution and the disks were dried overnight at 50 °C. Then, the bioassay, which was described in a previous publication, is performed. Very briefly: the SPCEs (DRP-110STR) were washed three times with 50 μL 50 mM PBS buffer (pH 7.4). Then, 10 μL of the capture AB (25 μg mL^{-1} in 50 mM PBS buffer, pH 7.4) were dropped onto the working electrode. For each step of the bioassay, incubation and washing were performed as follows: after incubation for 1 h at room temperature under water saturated atmosphere the solution was removed and the electrode washed three times with 50 μL PBST (50 mM PBS + 0.05% (w/v) Tween 20, pH 7.4). After drying under nitrogen flow, blocking was performed using 10 μL PBS blocking buffer (50 mM PBS + 1% (w/v) BSA, pH 7.4). In the third step, the antigen (AG) solution (100 ng mL^{-1} in 50 mM PBS, pH 7.4) was added and the dry probe AB disk was set on top. After incubation and washing, the electrodes were washed additionally with 50 mM PBS (pH 7.4) and double-distilled water. Directly prior to the electrochemical measurement, the electrode was dried under nitrogen flow.

Moreover, different oxygen scavengers were tested, which were added to the trehalose solution before drying of the disks (5 mM in 20% (w/v) trehalose solution), namely ascorbic acid (AA), sodium sulfite (Na_2SO_3) and sodium hydrogen carbonate ($NaHCO_3$).

2.4. Fabrication of flow chips

The flow chips consisted of a DRP-110STR electrode as bottom and a PMMA piece with in- and outlet as top. Both parts were glued together by double-sided adhesive tape in which the channel layout was cut (Fig. 2, a). The fabrication was done by a laser cutter with CO_2 laser (30 W, λ = 10.6 μm, image density 5) according to a previously designed template (Fig. 2, b). The channel layout (blue) was cut out of double-sided adhesive tape (100% power, 70% speed, 200 PPI) and glued to the SPCE after washing the electrode three times with 50 μL 50 mM PBS (pH 7.4) and drying under nitrogen flow. Then, the capture AB immobilization was performed as described for the standard bioassay above. For the top, the outline, in- and outlet (black) were cut out of PMMA (100% power, 6.5% speed, 1000 PPI) and the cavity (grey) was engraved in the bottom side of the PMMA (40% power, 90% speed, 1000 PPI). The cavity was between 75 and 100 μm deep.

For first experiments, the top was glued together with the SPCE after capture AB immobilization. For microchips with dried AB-AgNPs, blocking with 20 μL PBS blocking buffer (50 mM PBS + 1% (w/v) BSA, pH 7.4) was additionally performed with incubation and washing as described above for the bioassay and the electrodes were dried under nitrogen flow. Moreover, the PMMA tops were cleaned by plasma treatment for 1 min (0.2 bar, 75 W, 100% O_2) and 10 μL of 10% (w/v) trehalose in AB-AgNPs stock solution (in 10 mM HEPES + 0.1% (w/v) BSA) were pipetted into the cavity on the bottom side of the PMMA top and dried overnight at 50 °C. The top and bottom part were glued together to form the finished flow chip. All chips were sealed using tape and stored at 4 °C until further usage.

2.5. Microfluidic experiments

As pre-test, the AB-AgNP stock was diluted 1:2 with a 0.2 M KCl solution. Then, 50 μL of this mix were pipetted on a DRP-110

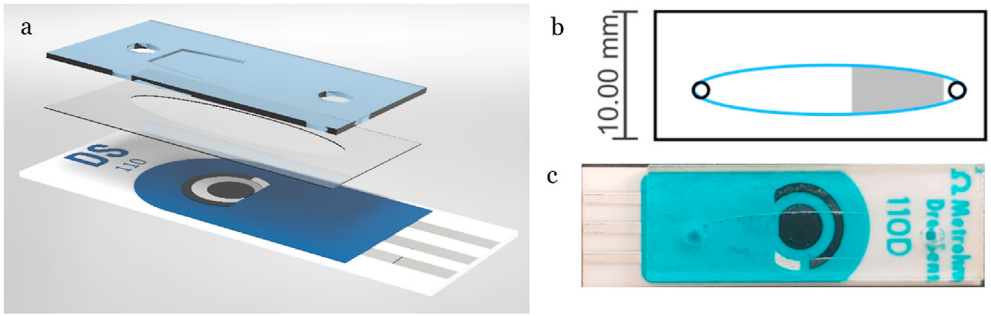

Fig. 2. Schematic representation of the three-layered flow chip (a) with DRP-110STR as bottom layer, double-sided adhesive tape (transparent, 100 μm thickness, middle layer) and PMMA top (blue). Template for the laser cutter (b), while black lines were cut out of PMMA (100% power, 6.5% speed, 1000 PPI), blue oval was cut out of double-sided adhesive tape (100% power, 70% speed, 200 PPI) and grey was engraved into PMMA (40% power, 90% speed, 1000 PPI) and actual photograph of the finished microfluidic chip (c) with scale bar representing 10.00 mm [Colors should be used in print]. (For interpretation of the references to color in this figure legend, the reader is referred to the Web version of this article.)

electrode, covering the three-electrode area, and the electrochemical measurement was performed: pretreatment with 1.25 V for 60 s and −0.8 V for 30 s, DPV from −0.25 V to 0.25 V with t_{puls} = 50 ms, E_{step} = 10 mV, $E_{amplitude}$ = 80 mV, scan rate = 20 mV s^{-1}. As comparison, a DRP-110 was glued together with the channel top consisting of structured double-sided adhesive tape and a PMMA piece with in- and outlet. The channel was filled with the mix (0.01 mg mL^{-1} AB-AgNP in 0.1 M KCl) via manual withdrawal of the solution out of an Eppendorf cup from the opposed side with a syringe and the electrochemical measurement was performed again.

First microfluidic experiments were performed using the setup shown in Fig. S2 (a), while the flow chips with dried AB-AgNPs were operated using a simplified version (Figs. S2 and b). The pumping strategy for microfluidic experiments with and without dried AB-AgNPs is shown in Fig. S3. The system was kept bubble-free at any time and for the experiments with AB-AgNPs in solution (a), the AG was incubated with the AB-AgNP in a 1:1 ratio for 2 h prior to injection. For electrochemical detection, the channel was filled with 0.1 M KCl, removed from the chip holder and inserted into a Bluetooth potentiostat. As pretreatment 1.18 V for 60 s and −0.8 V for 30 s were applied before DPV was performed from −0.25 V to 0.25 V with t_{puls} = 50 ms, E_{step} = 10 mV, $E_{amplitude}$ = 80 mV, scan rate = 20 mV s^{-1}.

The bioassay was repeated over six months to test the stability of the dried reagents. For these measurements a 10% (w/v) trehalose with 10 mM Na_2SO_3 solution was used as matrix to dry the AB-AgNP solution (20 μg mL^{-1}) overnight at 50 °C.

3. Results and discussion

3.1. Development of AB-AgNPs as dry reagent for sensors and microfluidic chips

In previous work, a bioassay for NT-proBNP using AgNPs and SPCEs was developed as described in the introduction [12]. Here, detailed information on the electroanalytical principle for AgNP detection via DPV are described, as well as development and optimization of the bioassay and its corresponding parameters. Limits of detection of 4.0 ng mL^{-1} were achieved, making the bioassay well-suited for NT-proBNP testing being just slightly above the 1 ng mL^{-1} clinical threshold. However, the multiple assay steps, pipetting and incubation periods as well as reproducibility and the need for all liquid reagents, rendered this assay merely a proof-of-principle bioassay. Instead, we investigated here, how a general immune sandwich assay for an important biomarker can be translated into a self-contained, miniaturized biosensor, focusing on a microfluidic format, which would allow FIA-like automation. The used antibodies (biotinylated polyclonal capture AB and monoclonal probe AB) are included in the commercially available NT-proBNP test by Roche Diagnostics [19]. Therefore, the specificity and binding efficacy of this AB pair was adopted without further tests. Initial tests investigated the possibility of drying AgNP-labeled probe antibodies (AB-AgNPs). Here, the functionality of the antibodies as well as the nanoparticle colloidal stability have to be maintained throughout the process of drying and redispersion. First, 20 μL AB-AgNPs were dried on a polymer support using different rehydration times (Figs. S4 and a). Using 20 μL HEPES, the optimum signal was achieved after incubation of the disk for 1 h. The redispersion was not complete after 30 min, while after 2 h, beginning oxidation of the AB-AgNPs by air oxygen decreased the signal again. When compared to control AB-AgNPs in solution (Figs. S4 and b), it was observed that drying has only minor influence on the electrochemical activity, suggesting that the rehydrated AB-AgNPs do not form clusters that would impeded in their electrochemical quantification. The increased signal variability is assumed to be caused by the larger number of steps taken prior to signal generation. However, storage of the dehydrated AB-AgNPs revealed instability over time (Fig. 3, a), dropping to only 20% of the original peak area after one week due to oxidation of the silver by air oxygen. AB-AgNPs were therefore sought to be embedded in a matrix, which should dramatically decrease oxidation and hence increase long-term stability. For simple rehydration in microfluidic channel and to maintain the stability of the attached antibodies, main design criteria for the matrix were solubility in water/buffer, complete dehydration at ≤50 °C, and no interference with the NPs, antibodies or the electrochemical measurement. Thus, agarose as a hydrogel with large pore sizes was studied (0.1–0.5% (w/w) agarose in double-distilled water) with various drying procedures. The strong yellow color of all gels indicates that the AB-AgNPs do not aggregate upon drying. Less concentrated gels show a slight color shift to orange after several days, while the 0.5% (w/w) agarose gel stays yellow. Since the AgNPs turn orange/brownish upon oxidation [20], this refers to an increased stability against oxidation for higher concentrated agarose gels. However, it was not possible to recover the AB-AgNPs by passive diffusion independent of the agarose content used. It is assumed the pores are too small for the 50 nm NPs to migrate just based on diffusion. A second, promising approach is the use of sugars such as maltose and trehalose which are often employed in freeze-drying of proteins. Specifically, trehalose is well known to stabilize biomaterials due to interactions of the sugar with polar head groups and glass formation [21]. While establishing a glass-like network upon drying, it completely dissolves by addition of water. Experiments showed that AB-AgNPs

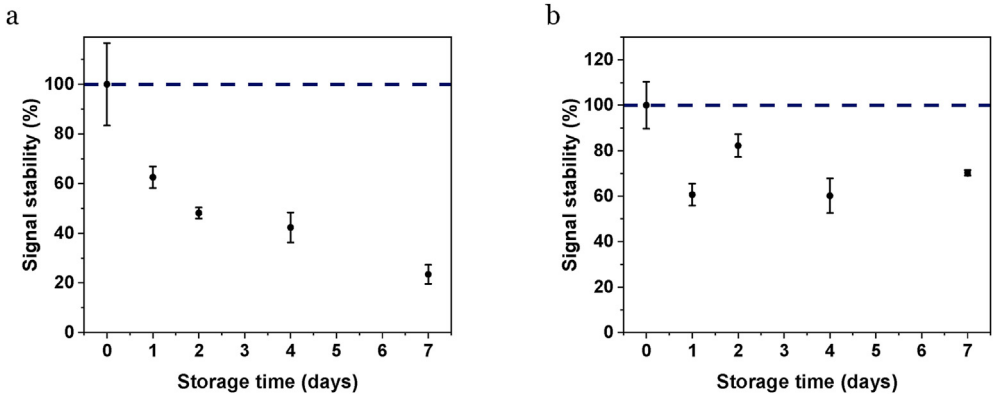

Fig. 3. Signal stability of the dried AB-AgNPs without matrix (a) and in 20% (w/v) trehalose (b) over a week. Signal stability is calculated by normalizing the mean peak area of the respective day to the mean signal directly after drying. Standard deviations were calculated based on three parallel measurements of three separate disks. Error bars represent mean values $\pm 1\sigma$.

dissolved in trehalose solution and those first dehydrated in trehalose and then redispersed gave the same electrochemical response (Fig. S5). Furthermore, the electrochemical activity remained stable over a course of 7 days, after an initial drop of to 75% of the fresh AB-AgNP signal (Fig. 3, b).

It can be concluded that the matrix stabilizes the AB-AgNPs against oxidation and the stability in dry-form can be enhanced drastically by drying of the particles in trehalose matrix. In a final confirmation assay, it was determined, whether the antibodies remain stable and functional upon the dehydration in trehalose. The AB-AgNPs were dried in 10% (w/v) trehalose overnight at 50 °C in order to ensure a complete dehydration. As it is shown in Fig. S6, the assay delivered a signal of 0.37 ± 0.08 V μA for 100 ng mL^{-1} which is comparable to previous experiments and confirms that the antibodies are active after drying and rehydration and the dried AB-AgNPs in trehalose can be used in order to simplify the bioassay protocol.

3.2. Development of a microfluidic chip for NT-proBNP

Microfluidic chips with integrated electrochemical detection were chosen for the automation and miniaturization of the bioassay. This dramatically reduces any pipetting step and increases the efficiency of the assay. The portable SPCE was integrated into microchannels through adhesive tape and laser cutting processes. Various channel shapes (Fig. S1) and heights were tested in order to avoid air bubble trapping and enable the wetting of the three-electrode area, while in the end the design shown in Fig. 2 with a channel height, *i.e.* tape thickness, of 100 μm showed superior performance. The overall functionality of the electrochemical detection strategy within microfluidic channels was proven by comparing the performance against a stand-alone SPCE electrode. The microdevice was filled manually with a 1:1 mixture of AB-AgNP stock solution and 0.2 M KCl, and the same solution was dropped on the stand-alone SPCE. It was found that while the peak height varies greatly between 28 ± 4 μA and 13 ± 1 μA, more importantly, the peak area is constant in the margin of the error (0.8 ± 0.1 V μA vs. 0.7 ± 0.1 V μA) (Fig. 4). Consequently, the same amount of silver is converted in both systems, but the thin layer and the partial coverage of the three electrodes due to the channel layout on the chip results overall in slower reactions and an increased peak width.

The reduced counter electrode surface area within the microchannel with respect to the working electrode area resulted in suboptimal electrochemical conditions, *i.e.* gas evolution occurred

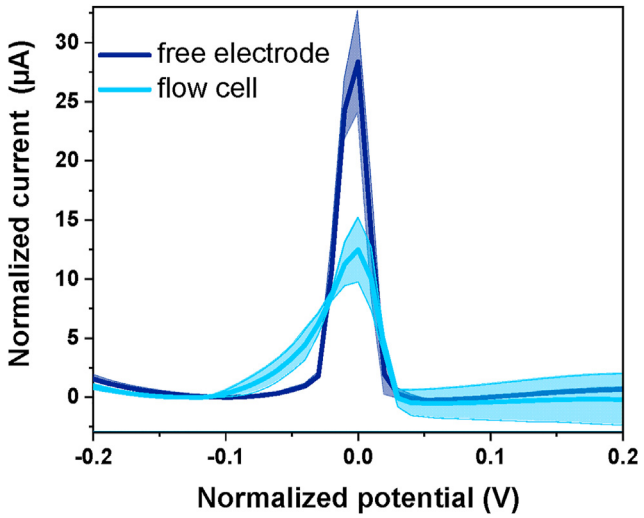

Fig. 4. Differential pulse voltammograms of a 1:1 mixture of AB-AgNP stock and 0.2 M KCl on a free DRP-110 (dark blue) or in a microfluidic channel (light blue), normalized to the respective current at −0.12 V in y-direction and to the peak potential in x-direction. The colored area behind the curve represents standard deviation calculated based on three parallel measurements (n = 3). (For interpretation of the references to color in this figure legend, the reader is referred to the Web version of this article.)

during the oxidative pre-treatment at 1.25 V. By lowering this oxidation potential to 1.18 V, bubble-free processes could be ensured, which is important for the reliability of the assay. It should be noted, that another strategy could be the design of a larger counter electrode to fit within the channel in the future. Using the current design and electrochemical strategy, a microfluidic chip bioassay was performed by immobilization of the capture AB in the flow chip and injection of pre-incubated AG/AB-AgNP mix resulting in a LOD 15x lower compared to the stand-alone sensor (Fig. S7). We assume this is due to the lowered diffusion effects of the nanoparticles within the narrow confinement of the microchannels, and the more effective washing that can be done reducing non-specific binding. At the same time, the mean standard deviation ($\bar{\sigma}$) is with 25% ($n \geq 4$) too high. Therefore, the trehalose drying procedure of AB-AgNPs was adapted from being an off-chip reagent to be directly deposited within the microchannels. Since drying within the channel itself lead to clogging (Fig. S1) a cavity was created in the PMMA top to still dry the AB-AgNP directly within the chip. Different depths (50–100 μm) and

volumes of AB-AgNP trehalose mix (5 and 10 μL) were tested. The focus was on obtaining a deep enough cavity to assure penetrability of the microchannel with as much AB-AgNP trehalose mix as possible without it spreading over the PMMA top before drying. Also to ensure complete dissolution of the AB-AgNPs, the cavity was kept as shallow as possible. With 40% laser power, which results in a cavity depth around 87 μm, reliable permeability was reached. Moreover, an oxygen plasma treatment (1 min, 75 W) was added to increase hydrophilicity of the PMMA and facilitate even spreading of the solution inside the cavity. Also, for the successful and reproducible release of the nanoparticle conjugates three washing buffers (PBST, PBST + 0.1% (w/v) BSA and PBST +0.1 M KCl) and various incubation and washing velocities were investigated (Fig. S8). The highest signal and also highest signal-to-noise ratio was obtained by using 0.5 μL min^{-1} for rehydration of the AB-AgNPs and incubation with the sample, and washing with 750 μL PBST at 50 μL min^{-1}.

3.3. Performance of the microfluidic bioassay

Finally, using the optimized conditions, dose-response curves for NT-proBNP were carried out both in buffer and undiluted human serum (Fig. 5). For the measurements in buffer (a), a LOD comparable to the biochip with liquid AB-AgNP reagent was obtained (0.24 ng mL^{-1}) confirming the superiority of the miniaturized biosensor in comparison to the stand-alone bioassay with a LOD of 4.0 ng mL^{-1}. The optimized microchip assay is drastically simplified as only one pump is required. Thus, by having reduced assay steps, avoiding manual pipetting, and preventing non-specific interactions, this optimized microfluidic biosensor has only 9% error ($n \geq 3$) in contrast to the prior microchip without dried AB-AgNPs ($\bar{\sigma}$ =25%) and the stand-alone bioassay ($\bar{\sigma}$ =17%). This suggests that the assay is highly suitable for the automation in a flow injection setup, both in a POCT as well as a clinical lab system, which would further decrease the variability and increase parallelization and efficacy. Here, an in-line injection port for the sample and KCl solution could be used with washing buffer as flow stream which will be the focus of future studies.

In spiked human serum (b), the course of the dose-response curve is analogous to experiments done in buffer, providing a LOD of 0.57 ng mL^{-1} and a mean standard deviation of only 6% ($n \geq 3$). The slightly lower sensitivity was expected due to partial blocking of the electrode by serum protein adsorption. Overall, it can be concluded that this microchip biosensor is suitable for the analysis of NT-proBNP content in blood. To confirm the results obtained by our microfluidic assay, the spiked serum samples, which were obtained from Roche Diagnostics, were additionally analyzed with Roche's Elecsys®. The results with corresponding divergence between NT-proBNP spike concentration (β_{spike}) and actual concentration determined with the Elecsys system ($\beta_{Elecsys}$) are shown in Table 1.

The reason for the rather big divergence between spiked concentration and concentration found with the Elecsys® system is known to be the dissolution of the peptide out of the matrix. This causes a decrease in peptide stock concentration. Taking this commercially available analysis as the gold standard and the real concentration of NT-proBNP, the data from the serum calibration can be fitted again (Fig. S9) and a new LOD, which is even below the previously determined one, can be calculated. With a NT-proBNP concentration of 0.38 ng mL^{-1}, this LOD is only 37% higher than the one calculated in buffer. It can be concluded that the protein adsorption on the electrode has only minor influence on the assay and also the antibody binding is not changed.

Various NT-proBNP tests have been published in recent years, as further discussed in Ref. [22]. A recent study by Pollok et al. [3] is technologically closest to our microfluidic biosensor. Their reported LODs are similar, however our sensor includes a simpler working procedure and smaller sample volume (10 μL vs. 100 μL). Moreover, the developed method shows distinct advantages compared to the currently used methods in clinical settings such as the commercially available NT-proBNP tests from Roche Diagnostics. With the Cobas h 232 a portable point-of-care device with optical detection of AuNP labels is offered [19]. However, typical for lateral-flow-assays larger sample volumes are needed, which makes it impossible for use in home-monitoring. In contrast, the here developed microchip assay only needs 10 μL of sample volume, which can easily be obtained via a mere finger prick. Secondly, fleece and

Table 1
NT-proBNP spiked concentrations (β_{spike}) as obtained from Roche Diagnostics with respective NT-proBNP concentrations measured with Roche's Elecsys® ($\beta_{Elecsys}$) and divergence of both.

β_{spike} (ng·mL^{-1})	$\beta_{Elecsys}$ (ng·mL^{-1})	Divergence
1.00	0.81	18.68%
3.00	2.32	22.56%
10.00	8.01	19.91%
30.00	27.50	8.30%
100.00	42.77	57.23%

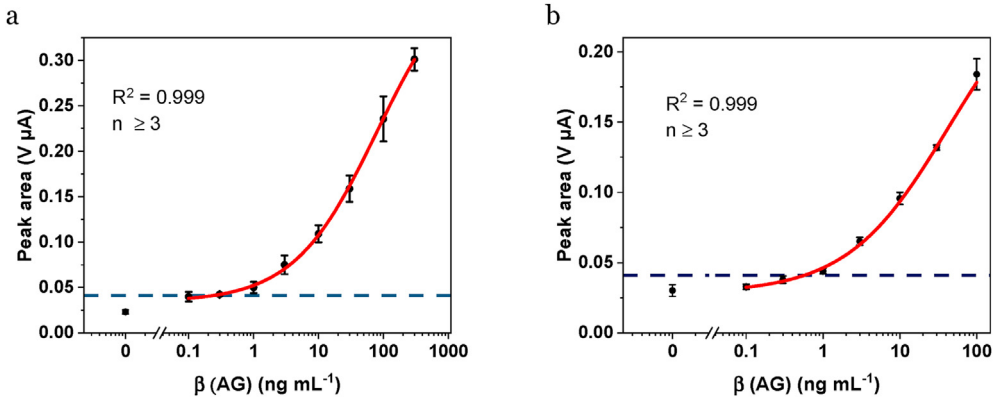

Fig. 5. Plot of peak area against logarithm of antigen concentration in PBS buffer (50 mM, pH 7.4, a) and undiluted human serum (b) with logistic fit (red line) and corresponding parameters. The blue dashed line indicates the LOD. Standard deviations were calculated based on four parallel measurements using four different flow chips, while outliers were removed after Q-test (confidence interval 95%). Error bars represent mean values ±1σ ($n \geq 3$). (For interpretation of the references to color in this figure legend, the reader is referred to the Web version of this article.)

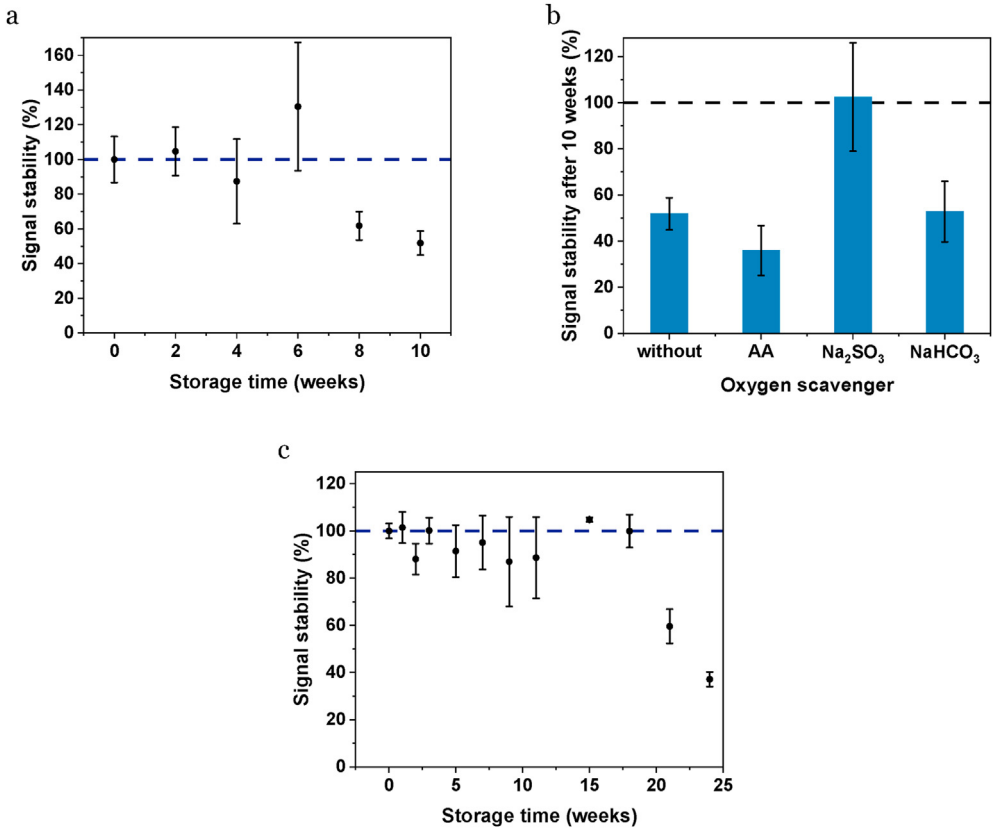

Fig. 6. Stability of the bioassay signal using the AB-AgNPs, dried in 10% (w/v) trehalose at 50 °C overnight, stored at 4 °C over ten weeks (a). Signal stability after ten weeks using none or different oxygen scavengers (5 mM, ascorbic acid (AA), sodium sulfite and sodium hydrogen carbonate)(b). Standard deviations were calculated based on five parallel measurements on five different SPCEs, while outliers were removed after Q-test (confidence interval 95%). Error bars represent mean values $\pm 1\sigma$ ($n \geq 4$). Stability of the bioassay signal using the AB-AgNPs, dried in 10% (w/v) trehalose with 10 mM sodium sulfite at 50 °C overnight, stored at 4 °C over six months (c). Standard deviations were calculated based on four parallel measurements on four different flow chips, while outliers were removed after Q-test (confidence interval 95%). Error bars represent mean values $\pm 1\sigma$ ($n \geq 3$). In all cases, the bioassay was performed in the microfluidic flow chip using a constant AG concentration of 100 ng mL^{-1} and signal stability means peak area normalized to the signal right after drying.

membrane fabrication for LFA test strips are prone to variations requiring a continuous fine-tuning of products made during the manufacturing process, so that other assay formats are highly desirable. The Cobas h 232 has a measuring range from 0.06 to 9 ng mL^{-1} and a detection time of 12 min, which makes it superior with respect to analytical performance. However, the here presented assay is with its dynamic range from 0.6 to 100 ng mL^{-1} sensitive in the necessary range for chronical heart failure and will most likely gain from better manufacturing strategies once designed for mass production, just as the Cobas system [4]. Another NT-proBNP detection device is Roche's Elecsys®, which is designed for analytical laboratories [18]. Here, NT-proBNP in blood serum or plasma is detected via electrochemiluminescence. The immunoassay is performed with 15 μL sample volume in a disk or rack handling system. The analytical performance is with a measuring range of 5–35,000 ng L^{-1} and 9–18 min assay time clearly superior. However, this detection system is a lab device, which is expensive, requires sample preparation and cannot be used at the point-of-care.

3.4. Stability study

AgNPs are known to be easily oxidized under ambient conditions, leading to a perception of instability especially for long-term uses in the scientific literature [23]. However, we have previously demonstrated, that protein-coated AgNPs remain colloidally stable over ten weeks and deliver a constant electrochemical signal for at least four weeks when stored at 4 °C, indicating that long-term stability is clearly achievable. The here developed trehalose-supported drying of AB-AgNPs also showed significantly improved performance (see Fig. 3), however, when monitoring the trehalose disks over ten weeks (Fig. 6, a), it is obvious that storage beyond 4 weeks is not feasible as the predictable oxidation of the AgNPs leads to unreliable and eventually only limited signal responses (i.e. drop to 50% of the original signal). To improve long-term stability of the dried AB-AgNPs, various oxygen scavengers were included in the trehalose matrix. Specifically, before drying, 5 mM ascorbic acid (AA), sodium sulfite (Na_2SO_3) or sodium hydrogen carbonate ($NaHCO_3$) were added to the trehalose mix, respectively. None of those substances showed a negative effect on the original electrochemical signal of the bioassay. After ten weeks, the assay was performed again to determine their protective power against oxidation (Fig. 6, b). While ascorbic acid and $NaHCO_3$ showed no protective effect, Na_2SO_3 was highly effective in avoiding any oxidation of the AgNPs and hence a normalized signal of 100 ± 23% was obtained. This indicates that Na_2SO_3 is indeed suitable to protect the AgNPs from oxygen, while having no negative influence on the bioassay itself.

Therefore, the AB-AgNPs were dried in trehalose with 10 mM Na_2SO_3 within the microchips. After assembly, the chips were sealed for storage at 4 °C, where a constant humidity in the channel could best ensure similar conditions for all dried AB-AgNPs. Finally,

the signal stability over four months was investigated (Fig. 6, c).

Here, over a period of 18 weeks, the bioassay signal stays constant with a mean relative error of 10%. This is a key finding as it supports the general feasibility of dry storage of protein-coated AgNPs in air. Afterwards, the signal decreases rapidly and reaches 30% at six months. It is assumed, that this drop is due to the depletion of the oxygen scavenger. For an extension of the AB-AgNP stability in dry form, a higher oxygen scavenger concentration will simply be used in the trehalose matrix in the future. The high relative errors for weeks 9 and 11 of around 20% can be explained by handling errors and the small number of replicates of hand-made flow chips that were used.

4. Conclusion

Overall, we presented here a method for NT-proBNP detection ready for the challenges of the POC.The electrochemical detection via silver nanoparticle labels in a microfluidic chip provides the appropriate limit of detection, dynamic range and through the selection of antibodies also specificity needed for a point-of-care test system, where a finger prick sample volume must suffice. The most important design criteria were the reduction in sample colume needed and the one-step assay procedure as typically afforded by lateral-flow assays (LFAs). The former was accomplished through a microfluidic design that can provide reliable data using only 10 μL of sample volume. The latter was obtained through dry-storage of the electrochemical label, AgNPs, on chip. The decision to investigate microfluidic channel designs instead of a membrane-based system in LFAs stems from the unavoidable variability of membrane and fleece fabrication that is a ubiquitous challenge in the rapid test community. Furthermore, each LFA concept must use enough colume to saturate the membrane material which either requires two-step procedures or large sample volumes. We demonstrated here therefore the proof-of-principle that membrane-free systems can provide the analytical figures of merit necessary for sensitive NT-proBNP detection for the POC.

Moreover, the research demonstrated that AgNPs are not only colloidally stable, but can also be rendered highly durable against oxidation by dehydrated storage in the presence of an oxygen scavenger. This opens up further possibility for their use as label in a many other electrochemical and possibly also optical POCTs for clinical diagnostics of low-concentrated analytes that can currently not be served with standard LFA technology.

CRediT authorship contribution statement

Franziska Beck: Conceptualization, Investigation, Writing – original draft, Formal analysis, Visualization. **Carina Horn:** Resources, Supervision, Funding acquisition, Project administration. **Antje J. Baeumner:** Conceptualization, Resources, Writing – review & editing, Supervision, Funding acquisition, Project administration.

Declaration of competing interest

The authors declare that they have no known competing financial interests or personal relationships that could have appeared to influence the work reported in this paper.

Acknowledgements

We thank Vanessa Tomanek for her help with Figs. 1 and 2.

Appendix A. Supplementary data

Supplementary data to this article can be found online at https://doi.org/10.1016/j.aca.2021.339375.

References

[1] G. Savarese, L.H. Lund, Global public health burden of heart failure, Card. Fail. Rev. (2017) 7, https://doi.org/10.15420/cfr.2016:25:2, 03.
[2] S.A. Hunt, W.T. Abraham, M.H. Chin, A.M. Feldman, G.S. Francis, T.G. Ganiats, et al., ACC/AHA 2005 guideline update for the diagnosis and management of chronic heart failure in the adult: a report of the American college of cardiology/American heart association task force on practice guidelines (writing committee to update the 2001 guidelines for the evaluation and management of heart failure): developed in collaboration with the American college of chest physicians and the international society for heart and lung transplantation: endorsed by the heart rhythm society, Circulation 112 (2005) e154–235, https://doi.org/10.1161/CIRCULATIONAHA.105.167586.
[3] N.E. Pollok, C. Rabin, C.T. Walgama, L. Smith, I. Richards, R.M. Crooks, Electrochemical detection of NT-proBNP using a metalloimmunoassay on a paper electrode platform, ACS Sens. 5 (2020) 853–860, https://doi.org/10.1021/acssensors.0c00167.
[4] H.-N. Kim, J.L. Januzzi, Natriuretic peptide testing in heart failure, Circulation 123 (2011) 2015–2019, https://doi.org/10.1161/CIRCULATIONAHA.110.979500.
[5] V.L. Roger, Epidemiology of heart failure, Circ. Res. 113 (2013) 646–659, https://doi.org/10.1161/CIRCRESAHA.113.300268.
[6] C. Mueller, K. McDonald, RA.de Boer, A. Maisel, J.G.F. Cleland, N. Kozhuharov, et al., Heart Failure Association of the European Society of Cardiology practical guidance on the use of natriuretic peptide concentrations, Eur. J. Heart Fail. 21 (2019) 715–731, https://doi.org/10.1002/ejhf.1494.
[7] K.-S. Song, S.B. Nimse, M.D. Sonawane, S.D. Warkad, T. Kim, Ultra-sensitive NT-proBNP quantification for early detection of risk factors leading to heart failure, Sensors (2017), https://doi.org/10.3390/s17092116.
[8] F.G. Bellagambi, C. Petersen, P. Salvo, S. Ghimenti, M. Franzini, D. Biagini, et al., Determination and stability of N-terminal pro-brain natriuretic peptide in saliva samples for monitoring heart failure, Sci. Rep. 11 (2021) 13088, https://doi.org/10.1038/s41598-021-92488-2.
[9] Z. Pu, C. Zou, R. Wang, X. Lai, H. Yu, K. Xu, D. Li, A continuous glucose monitoring device by graphene modified electrochemical sensor in microfluidic system, Biomicrofluidics 10 (2016) 11910, https://doi.org/10.1063/1.4942437.
[10] E. Primiceri, M.S. Chiriacò, F.M. Notarangelo, A. Crocamo, D. Ardissino, M. Cereda, et al., Key enabling technologies for point-of-care diagnostics, Sensors (2018), https://doi.org/10.3390/s18113607.
[11] PRd Oliveira, M.M. Oliveira, A.J.G. Zarbin, L.H. Marcolino-Junior, M.F. Bergamini, Flow injection amperometric determination of isoniazid using a screen-printed carbon electrode modified with silver hexacyanoferrates nanoparticles, Sensor. Actuator. B Chem. 171–172 (2012) 795–802, https://doi.org/10.1016/j.snb.2012.05.073.
[12] F. Beck, C. Horn, A.J. Baeumner, Ag nanoparticles outperform Au nanoparticles for the use as label in electrochemical point-of-care sensors, Anal. Bioanal. Chem. (2021), https://doi.org/10.1007/s00216-021-03288-6.
[13] N. Hao, H. Li, Y. long, L. Zhang, X. Zhao, D. Xu, H.-Y. Chen, An electrochemical immunosensing method based on silver nanoparticles, J. Electroanal. Chem. 656 (2011) 50–54, https://doi.org/10.1016/j.jelechem.2011.01.029.
[14] J.C. Cunningham, M.R. Kogan, Y.-J. Tsai, L. Luo, I. Richards, R.M. Crooks, Paper-based sensor for electrochemical detection of silver nanoparticle labels by galvanic exchange, ACS Sens. 1 (2016) 40–47, https://doi.org/10.1021/acssensors.5b00051.
[15] C. Walgama, M.P. Nguyen, L.M. Boatner, I. Richards, R.M. Crooks, Hybrid paper and 3D-printed microfluidic device for electrochemical detection of Ag nanoparticle labels, Lab Chip 20 (2020) 1648–1657, https://doi.org/10.1039/d0lc00276c.
[16] H. Kanso, M. Begoña González García, S. Ma, R. Ludwig, P. Fanjul Bolado, D. Hernández Santos, Dual biosensor for simultaneous monitoring of lactate and glucose based on thin-layer flow cell screen-printed electrode, Electroanalysis 29 (2017) 87–92, https://doi.org/10.1002/elan.201600487.
[17] X. Li, K. Scida, R.M. Crooks, Detection of hepatitis B virus DNA with a paper electrochemical sensor, Anal. Chem. 87 (2015) 9009–9015, https://doi.org/10.1021/acs.analchem.5b02210.
[18] Roche Diagnostics AG. https://diagnostics.roche.com/ch/de/products/params/elecsys-nt-probnp.html#productSpecs. Accessed 9 Apr 2021...
[19] T. Bertsch, J.-P. Chapelle, C.-E. Dempfle, E. Giannitsis, M. Schwabs, R. Zerback, Multicentre analytical evaluation of a new point-of-care system for the determination of cardiac and thromboembolic markers, Clin. Lab. 56 (2010) 37–49.
[20] O.A.D. Gallardo, R. Moiraghi, M.A. Macchione, J.A. Godoy, M.A. Pérez, E.A. Coronado, V.A. Macagno, Silver oxide particles/silver nanoparticles interconversion: susceptibility of forward/backward reactions to the chemical environment at room temperature, RSC Adv. 2 (2012) 2923, https://doi.org/10.1039/c2ra01044e.
[21] L.M. Crowe, D.S. Reid, J.H. Crowe, Is trehalose special for preserving dry biomaterials? Biophys. J. 71 (1996) 2087–2093, https://doi.org/10.1016/S0006-

3495(96)79407-9.
[22] G. Colom, J.-P. Salvador, G. Acosta, F. Albericio, M. Royo, M.-P. Marco, Competitive ELISA for N-terminal pro-brain natriuretic peptide (NT-proBNP) determination in human plasma, Analyst 145 (2020) 6719–6727, https://doi.org/10.1039/d0an00650e.
[23] V.J. Keast, T.A. Myles, N. Shahcheraghi, M.B. Cortie, Corrosion processes of triangular silver nanoparticles compared to bulk silver, J. Nanoparticle Res. 18 (2016) 289, https://doi.org/10.1007/s11051-016-3354-9.